Effects of Droplet Size and Mass Loading on Water Mist Extinction

Ramagopal Ananth and John Hoover
Code 6183
US Naval Research Laboratory
Washington, DC 20375

INTRODUCTION

Water mist has been of great interest to the US Navy, as well as to the civilian fire protection community, as a replacement for Halon 1301. The latter, which has been the total flooding fire fighting agent of choice for many years, operates via a chemical mechanism by scavenging the free radicals that are the main species involved in combustion reaction chain propagation. Unfortunately, that mechanism also makes it a strong ozone-depleting agent in the atmosphere. As a result, Halon 1301 is being phased out by international treaty. Water mist, although it operates through a physical, rather than a chemical, mechanism, is one of the replacement agents currently being used or considered as a replacement.

The two-phase nature of water droplet extinction makes for an inherently more complex problem than was the case for Halon 1301. Effective suppression system designs must account for the size-dependent behavior of the droplets as they are injected and transported and the interaction of droplets with flames, which causes suppression through both evaporative cooling and oxygen dilution effects. Knowledge of the flame extinction concentrations is critical to this process.

Experimentally, one of the key tools for studying fire suppression has been the cup burner [Hirst and Booth], which is a co-flow diffusion burner having a coaxial cylindrical geometry as shown schematically in Figure 1. In the traditional application, a liquid fuel is introduced into the central cylinder and air, having an admixture of the gaseous fire suppression agent under study, is injected into the surrounding annulus. Cup burner experiments have been applied to the study of gaseous fuels with water mist as the suppression agent.

Because of the importance of cup burner studies, we have focused on simulating the dynamics of combustion in the cup burner illustrated in Figure 1. In previous work in our laboratory, the behavior of droplets having diameters below 32 micron was investigated [Ananth and Mowrey]. The current work extends those earlier results to larger droplets and higher fuel and air flow rates. The droplet sizes considered in the present simulations correspond to the typical droplet size range generated by water mist systems employed on Navy ships.

Simulations were performed on the SGI Altix Bx2 (eagle) and SGI Altix 4700 (hawk) High Performance Computing systems at the Air Force Research Laboratory, using the commercial Fluent 6.3 computational fluid dynamics software package.

THEORY

The axial symmetry of the cup burner was used to reduce the three-dimensional problem to two-dimensions (r and z) by neglecting transport along the φ axis. A further application of the symmetry condition reduced the domain by another factor of two. The resulting computational domain is shown in Figure 2.

The fluid phase was modeled using transient, Navier-Stokes equations with energy conservation. The discrete phase was simulated using Lagrangian methods; momentum coupling to the continuous phase was included, but radiation coupling between phases was not. In our prior work with smaller droplets, the interaction between the droplets and the radiation field was negligible. However, that may not be true for larger droplets and work is underway to incorporate droplet absorbance, emission and scattering into the simulations in order to determine the effects of droplet radiation on flame suppression.

Boundary conditions for the simulations are given in Table 1, where the boundary numbers correspond to the numbers in circles in Figure 2. The fuel was propane and the air was saturated with water vapor to prevent droplet evaporation prior to interacting with the flame. Boundaries were at 300 K, except for the fuel inlet and the lip of the inner wall, which were set to 600 K in order to simulate the heating that occurs at the edge of the cup in an actual burner.

The "trap" droplet condition at the inner wall lip caused all impacting droplets to flash into vapor, which is a reasonable approximation for a surface at that temperature. Droplets were allowed to escape at the air and fuel inlets as well as at the downstream end of the domain. In all cases, the droplets were injected into the co-flow air stream at the velocity of the air, which was increased, from the 0.10 m/s used in previous work, to 0.25 m/s in order to permit more massive droplets to reach the flame region. The fuel velocity was also increased by the same factor to maintain the same relative gas velocities.

A simplified propane-air combustion chemistry, based on the Gas Research Institute (GRI) 3.0 mechanism, was used. This chemistry involved 35 species and 217 reactions, including N_2 but excluding other nitrogen-containing species. The GRI chemistry was designed for natural gas, which is largely methane with a small admixture of propane and other species. Because the water mist suppression mechanism is primarily physical, rather than chemical, it was assumed that the details of the reaction chemistry would not play a critical role in the process and, therefore, that the same chemistry could be used for pure propane. That assumption is supported by the good agreement between experimental results and previous simulations in which GRI 3.0 was also used.

Time steps of 0.1 ms were used with data output at 100 step intervals, providing a temporal resolution of 10 ms. The initial simulations were run for a period of 2.35 s to allow the flame to stabilize before water droplets were injected; zero time for the results was set to the start of the

droplet injection period. Droplet injections were monodisperse and the mass was uniformly distributed across all cells of the air inlet.

RESULTS AND DISCUSSION

To date, simulations have been performed with 30, 50, 70, 90 and 100 micron droplets with total water (vapor plus droplet) mass fractions up to 0.38. For each droplet diameter, the water droplet loading was varied and the results were inspected to determine the concentration at which the flame was extinguished. The rate of Reaction 1(in kg/s) and the flame temperature (K) were used as metrics for suppression.

$$O + H_2 = OH + H \qquad \text{Rxn. 1}$$

In addition, the droplet concentration (kg/m^3) and the droplet tracks were plotted in order to help elucidate the mechanisms for extinguishment.

Because of the stepwise nature of the mass fraction variation, it is unlikely that these results correspond exactly to the critical extinction concentration. However, the values reported (the highest concentration that did not produce extinguishment and the lowest value that did cause extinguishment) bracket the actual critical value. In Figure 3, the bracket values are plotted for 30, 50 and 70 micron drops. For the 90 and 100 micron simulations, no extinguishment was observed in any of the simulations yet performed, so only lower limits are shown. For comparison, previous results for 8, 16 and 32 micron drops are included. The solid curve shown in Figure 3 is a visual indication of the trend, but is not intended to represent a functional relationship.

Good agreement with the previous work was obtained, with the slight differences in the region of overlap attributed to the increased air, fuel and droplet injection velocities in the current work. Based on these results, the most effective droplet diameter, in terms of mass fraction needed to produce extinguishment, is approximately 30 microns.

For droplet diameters of 30 microns or less, extinction initially occurs at the base of the flame, at the point of attachment to the burner, and the detached flame is expelled from the burner. This mechanism is seen in Figures 4 and 5 for the case of 30 micron droplets. Each frame in Figure 4 shows the reaction rate on the left and droplet tracks on the right. Note that the droplet tracks are color coded by arbitrary numbers representing the cell from which the droplet packet was originally injected. In Figure 5, flame temperature contours are on the left and droplet mass concentration contours on the right. The detachment effect is most clearly seen in the last three frames of Figure 5, in which a jet of droplet concentration has encroached on the flame near the base, causing the flame to lift off of the lip of the burner.

With droplet diameters of 50 microns and larger, the initial extinction is significantly above the point of attachment and the flame sheet is cut into two pieces. The upstream (detached) portion is

blown out of the simulation domain, just as in the case of smaller droplets. However, the lower (still attached) portion remains stable for a longer period. Figures 6 and 7 show the reaction rates, droplet tracks, flame temperatures and droplet concentrations for the 70 micron case. Again, the best illustration of the process is seen in the flame temperature contour plots (Figure 7), where it appears that the flame is essentially enveloped and smothered by the encroaching droplets. Note that the droplet concentration scale used in Figure 7 is six times that used in Figure 5.

This difference between the behavior of the smaller- and larger-droplet cases is believed to be caused by the reduced entrainment of the larger droplets into the base of the flame due to their greater inertia. The details of this behavior are under investigation. In addition, work is underway to reduce the bracket sizes for the 30 and 70 micron droplets and to locate the upper limits for the 90 and 100 micron droplets. Finally, as mentioned previously, work is underway to include coupling between the droplets and the radiation field to account for the effects of scattering, emission and absorbance of the droplets.

ACKNOWLEDGEMENTS

This work is supported by the Office of Naval Research, through the Naval Research Laboratory core program, and by the Department of Defense High Performance Computer Modernization Program, through the grant of time on the Air Force Research Laboratory SGI Altix Bx2 (eagle) and SGI Altix 4700 (hawk) systems.

REFERENCES

R. Hirst and K. Booth, *Fire Technol.*, 13(4), 296-315, 1977.

R. Ananth and R.C. Mowrey, *Combust. Sci. and Tech.,* 180, 1639-1692, 2008.

Boundary	Name	Boundary Conditions
1	Outlet	Pressure = 0.0 Pa Temp. = 300 K Fluid = 0.233 O_2 Droplet = Escape
2	Outer Wall	Slip = No Temp. = 300 K Droplet = Reflect
3	Axis	Symmetry
4	Fuel Inlet	Velocity = 0.05 m/s Temp = 600 K Fluid = 1.00 C_3H_8 Droplet = Escape
5	Inner Wall Lip	Slip = No Temp. = 600 K Droplet = Trap
6	Inner Wall	Slip = No Temp. = 300 K Droplet = Reflect
7	Air Inlet	Velocity = 0.25 m/s Temp = 300 K Fluid = 0.2288 O_2; 0.018 H_2O Droplet = Escape

Table 1. Simulation Boundary Conditions

For all gas compositions, the unspecified mass fractions are assumed to be nitrogen. All velocities are normal to the corresponding boundary. The droplet conditions are defined as follows:

Escape	Droplet is lost from the domain.
Reflect	Droplet bounces back into the domain and continues to be tracked.
Trap	Droplet immediately evaporates.

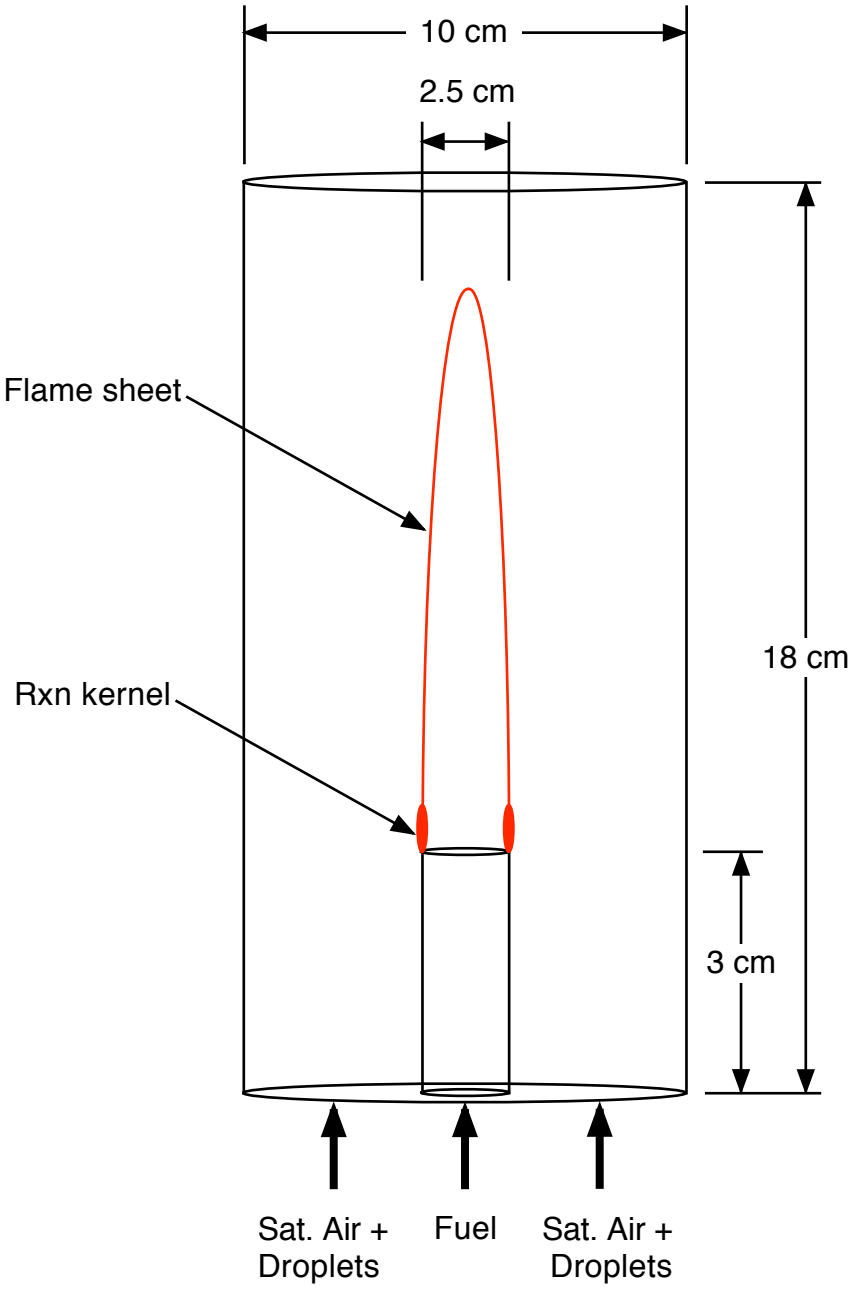

Figure 1. Cup Burner Schematic

The cup burner is a cylindrical, coaxial-flow, propane burner with the indicated dimensions. Typical flame sheets, together with their associated reaction kernel regions, are shown.

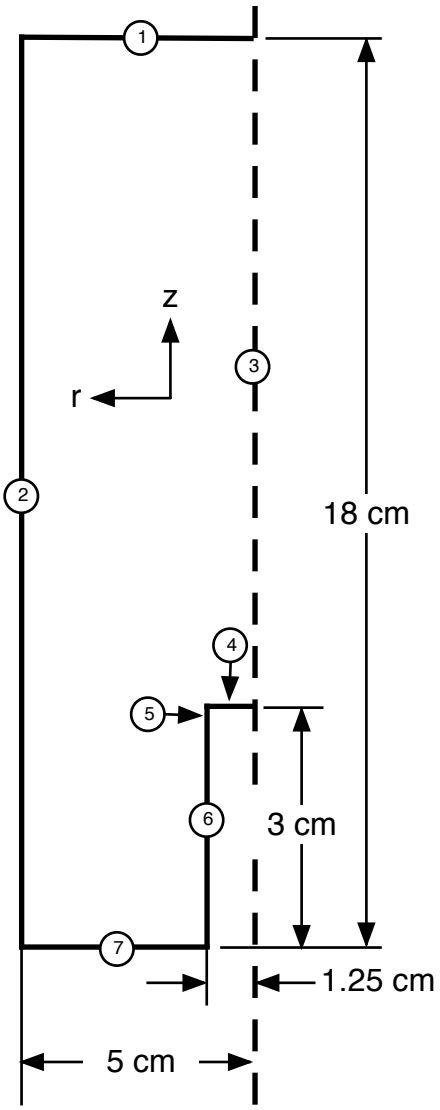

Figure 2. Simulation Domain

The symmetry of the problem was used to reduce the problem to the two-dimensional domain shown. The circled numbers refer to the boundaries listed in Table 1.

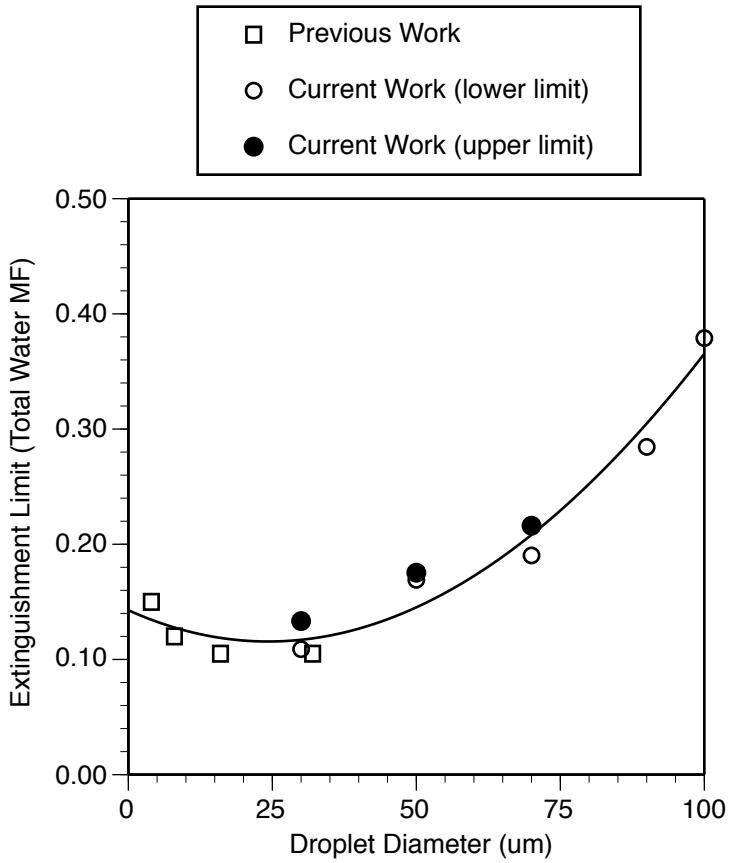

Figure 3. Extinguishment Limits vs. Droplet Diameter

Extinguishment limits are shown as the total water mass fraction (water vapor plus droplets) injected into the burner. Values for “Previous Work” are from Ananth and Mowrey. For “Current Work,“ the lower limits are the highest water mass fraction simulation that did not extinguish the flame while upper limits are the lowest water mass fraction simulation that did extinguish it.

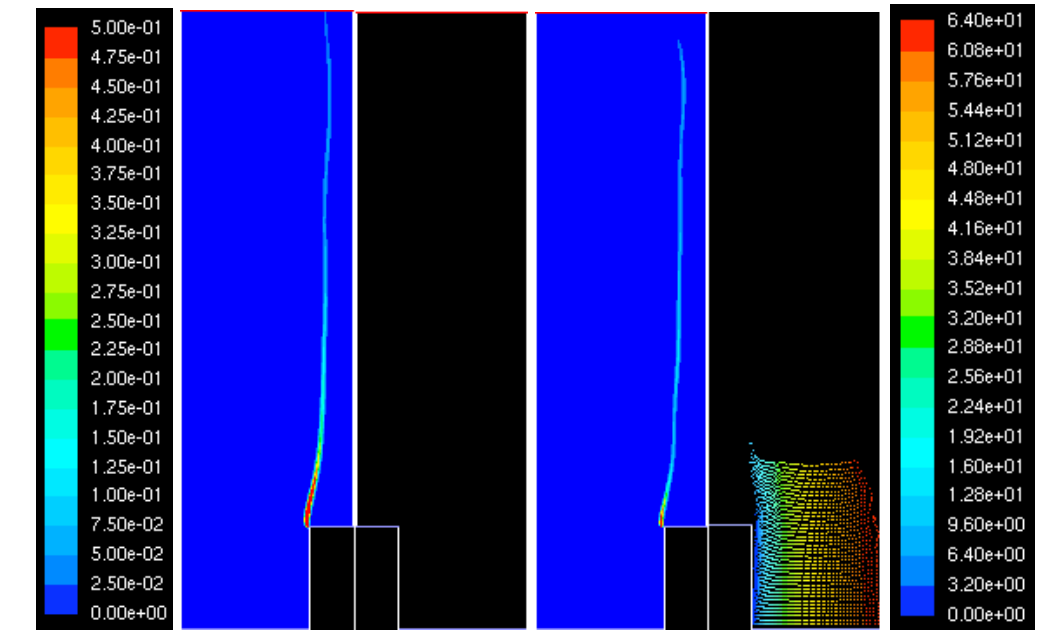

Rxn Rate (kg/s) 0.0 s 0.2 s Track ID

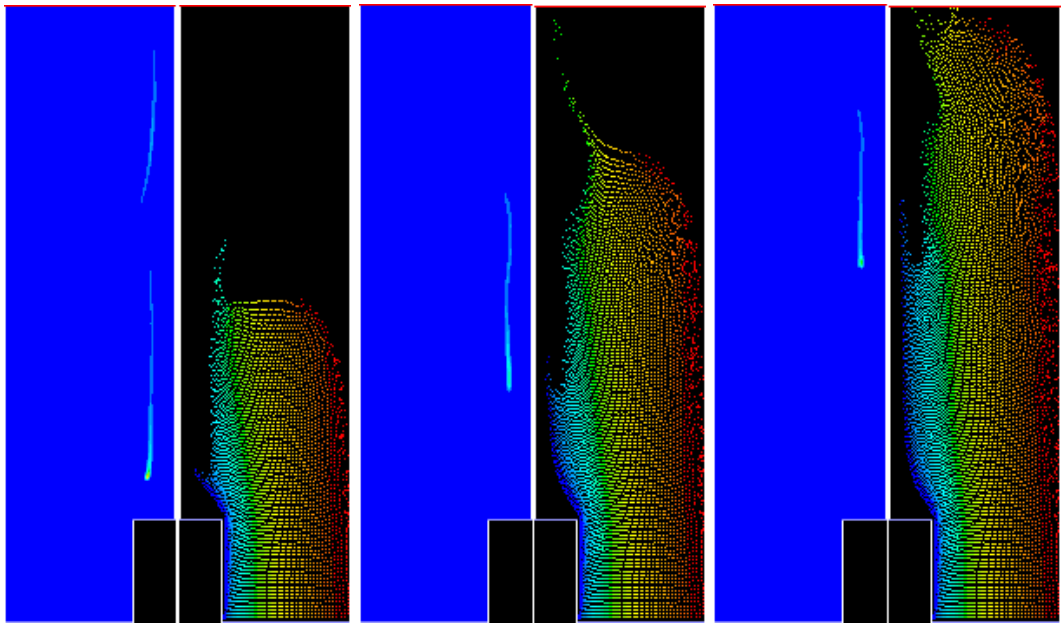

0.4 s 0.6 s 0.8 s

Figure 4. Reaction Suppression with 30 Micron Droplets

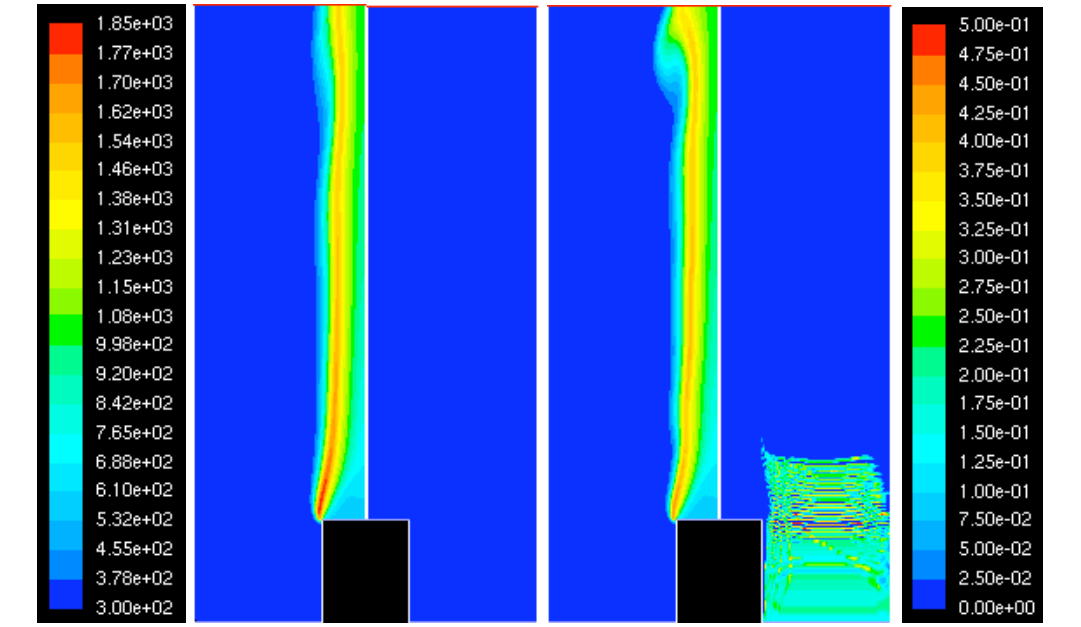

Temp. (K) 0.0 s 0.2 s Conc. (kg/m³)

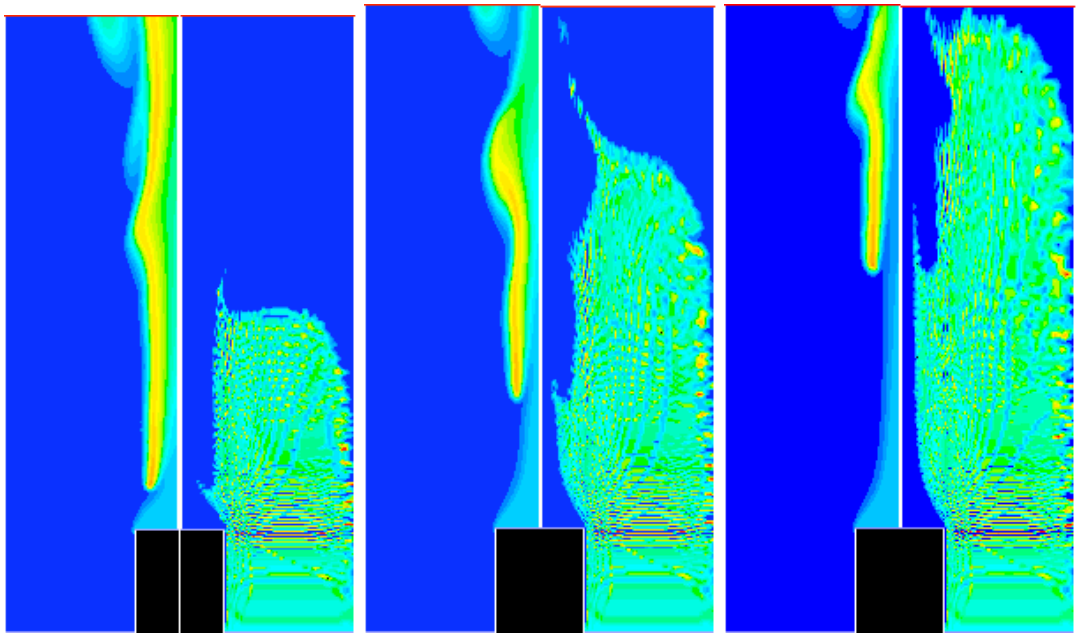

0.4 s 0.6 s 0.8 s

Figure 5. Temperature Suppression with 30 Micron Droplets

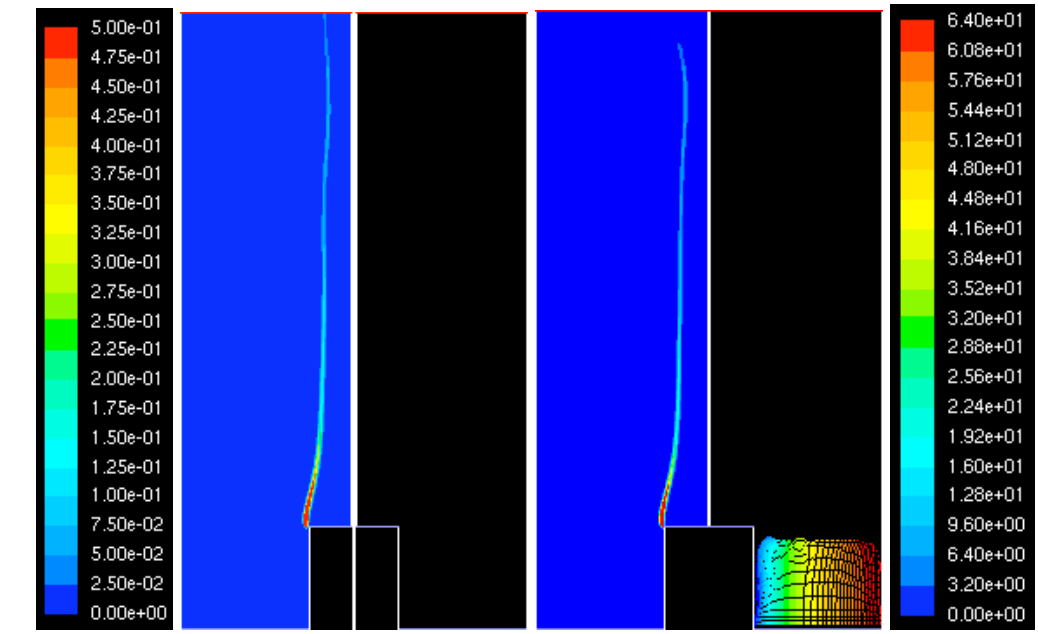

Rxn Rate (kg/s) 0.0 s 0.2 s Track ID

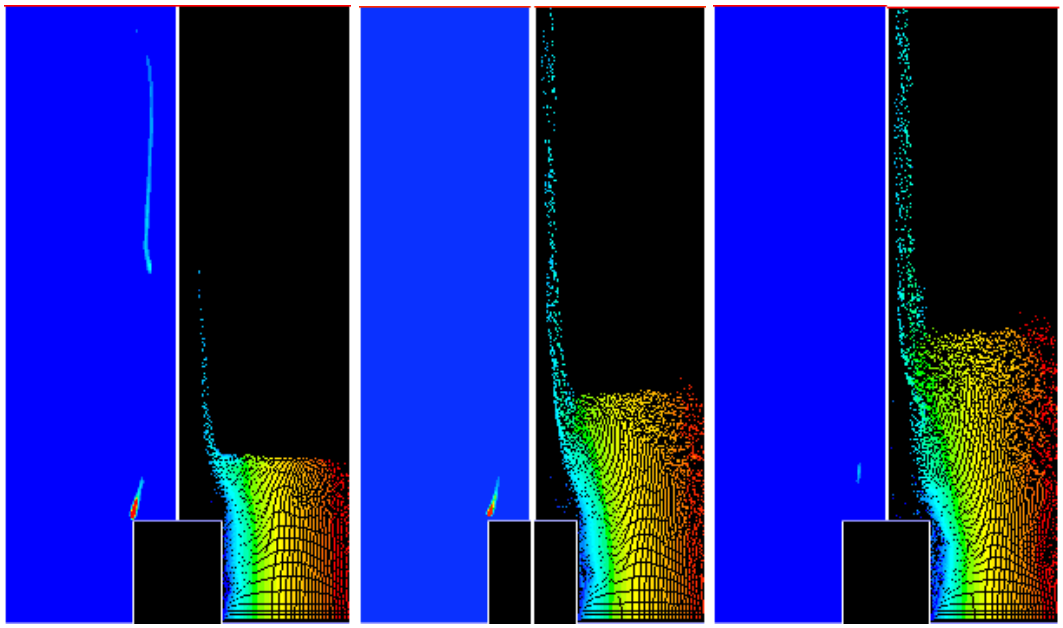

0.4 s 0.6 s 0.8 s

Figure 6. Reaction Suppression with 70 Micron Droplets

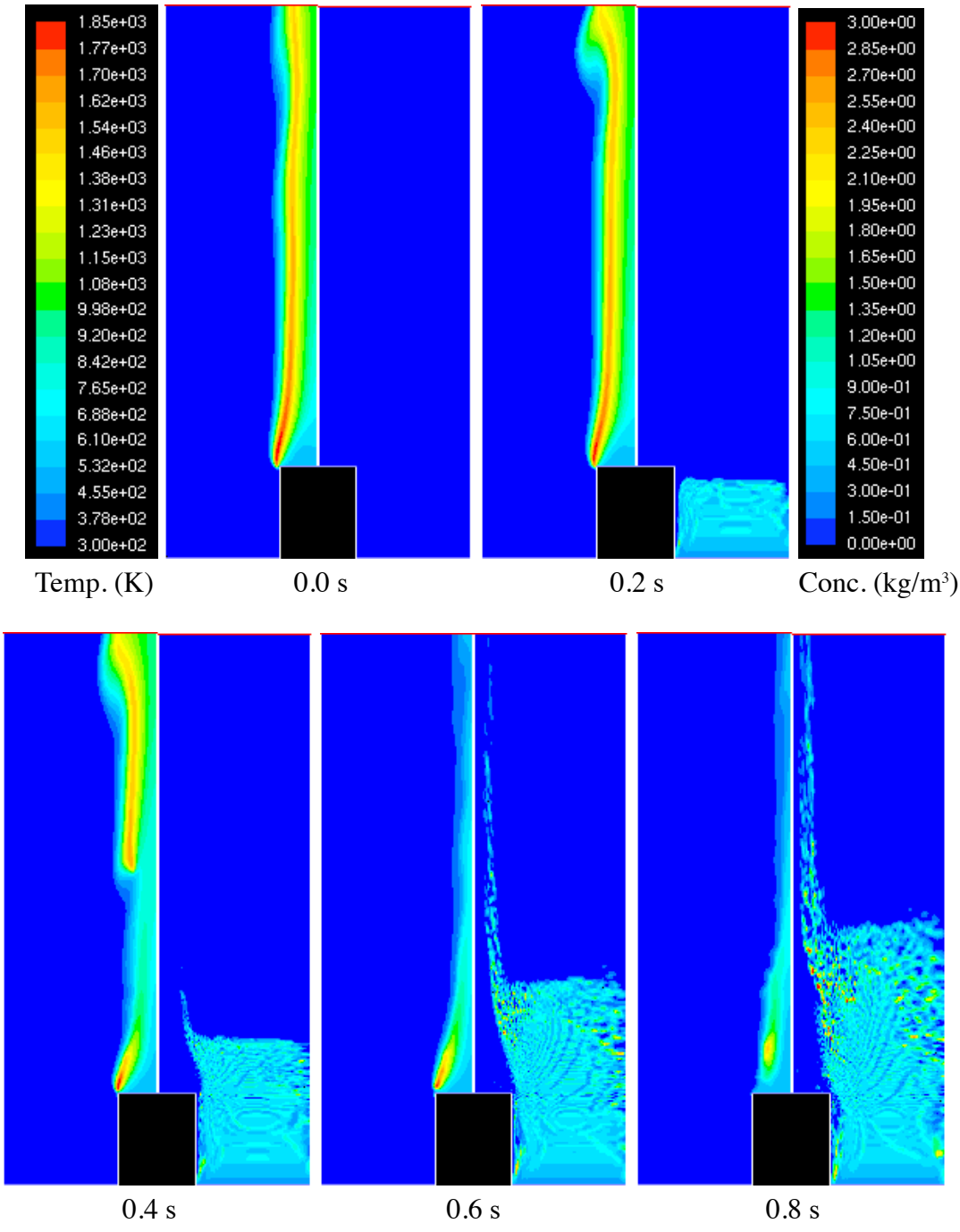

Figure 7. Temperature Suppression with 70 Micron Droplets

Note the difference in scales between the droplet concentrations in this figure as compared with Figure 5.